Biological Modification of Pentosans in Wheat B Starch Wastewater and Preparation of a Composite Film

Piwu Li
Shandong Academy of Sciences
Fei Zhao
Shandong Academy of Sciences
Xiaofeng Wei
Shandong Academy of Sciences
Xiangling Tao
Shandong Academy of Sciences
Feng Ding (bio_ding@126.com)
Shandong Academy of Sciences

Research article

Keywords: biological modification, chitosan, composite film, wheat pentosan

Posted Date: September 28th, 2021

DOI: https://doi.org/10.21203/rs.3.rs-942055/v1

Version of Record: A version of this preprint was published at BMC Biotechnology on January 17th, 2022.
See the published version at https://doi.org/10.1186/s12896-022-00734-w.

Biological Modification of Pentosans in Wheat B Starch Wastewater and Preparation of a Composite Film

Authors: Piwu Li, Fei Zhao, Xiaofeng Wei, Xiangling Tao, Feng Ding*

Institutional affiliations: School of Bioengineering, Qilu University of Technology, Shandong Academy of Sciences, Jinan, 250353, P.R. China; State Key Laboratory of Biobased Material and Green Papermaking (LBMP), Qilu University of Technology, Shandong Academy of Sciences, Jinan, 250353, P.R. China

Piwu Li and Fei Zhao contributed equally to this work.

*Corresponding authors: Dr. Feng Ding

Daxue Road 3501, Changqing District, Jinan 250353, P.R. China

E-mail: bio_ding@126.com

Abstract

Background: Petrochemical resources are becoming increasingly scarce, and petroleum-based plastic materials adversely impact the environment. Thus, an urgent need exists to replace petroleum-based materials with new and effective renewable materials.

Results: In this study, we isolated a wheat pentosan-degrading bacterium (MXT-1) from wheat-processing plant wastewater. The MXT-1 strain was identified using molecular biology techniques. We then analyzed the degradation characteristics of the bacteria in wheat pentosan. We found that wheat pentosan was effectively degraded by bacteria. The molecular weight of fermented wheat pentosan decreased from 1730 to 257 kDa. The pentosan before and after the biological modification was mixed with chitosan to prepare a composite film. After fermentation, the water-vapor permeability of the wheat pentosan film decreased from 0.2769 $g \cdot mm \cdot (m^2 \cdot h \cdot KPa)^{-1}$ to 0.1286 $g \cdot mm \cdot (m^2 \cdot h \cdot KPa)^{-1}$. The smooth and dense surface morphologies of the film was observed by scanning electron microscopy after fermentation. The tensile strength of the film decreased after fermentation modification, whereas the flexibility increased.

Conclusion: The results of this study have proved that the modified pentosan film could be a potential candidate for edible packaging films.

Keywords: biological modification; chitosan; composite film; wheat pentosan

Background

Approximately 30% of all plastic products worldwide are used as packaging materials [1]. Petrochemical resources are becoming increasingly scarce, and petroleum-based plastic materials adversely impact the environment owing to their toxicity and non-degradability. Thus, petroleum-based materials should be replaced with new and effective renewable materials. Xylan-type hemicellulose from agricultural and forestry crops has been studied by many scholars as a biodegradable, edible film material. Currently, crop wastes such as rye flour, oats, and arabinoxylan in wheat bran have been studied extensively with the objective of preparing film materials [2]. In addition, arabinoxylan extracted from wheat flour has been used to prepare edible films [3].

Pentosans are non-starch polysaccharides and a type of hemicellulose that exists in the cortexes of different grains. In addition to starch and gluten, wheat is also rich in non-starch polysaccharides, most of which are pentosans [4]. Industrial production of wheat gluten generates 2.4×10^7 tons of starch wastewater every year. Because of its high viscosity, wastewater is difficult to treat using conventional sewage-treatment methods [5]. Wheat starch-processing wastewater can be used as a good source of pentosans. The recycling of wastewater can also improve the economic efficiency of factories and ease the problem caused by sewage discharge [6].

Data from previous studies have shown that pentosan has beneficial effects on health [7,8]. For example, arabinoxylan offers many benefits for human health, including cholesterol-lowering activity, anti-type II diabetes effects, mineral absorption

enhancement, stool-bulking effects, and prebiotic benefits [9]. Moreover, gluten-free bread made with pentosan can be used to relieve the symptoms of celiac disease [10].

Pentosans have attracted must attention as sources of hemicellulose. In recent years, many studies have evaluated the applications of pentosans as film materials [11]. Polysaccharide films used for food packaging can isolate the food from ambient oxygen, prevent moisture from evaporating, and preserve aroma and flavor. However, the application range of polysaccharide films is limited by their poor mechanical strength, stability, and toughness. Glucuronic acid/xylan films can be modified by plasticization. Adding 50% of the plasticizer improves the ductility of a film and ensures its flexibility [12]. Acetylized-arabinoxylan and bleach treatment can improve the moisture-barrier properties of the hemicellulose film [13]. Mixed films containing chitosan and xylan have good hydrophobic properties, tensile strength, and other mechanical properties [14]. In addition, the tensile strength of high-molecular-weight arabinoxylan films is significantly lower than that of low-molecular-weight films [15].

The content of pentosans in wheat flour is approximately 2%, and the content of water-soluble pentosans is approximately 0.5% [16]. To increase the utility of water-insoluble pentosans and improve the mechanical strength of polysaccharide films, the molecular weight of water-insoluble pentosans should be reduced [15]. Biological modification has major advantages over other modification methods. First, organic matter can be used to treat industrial wastewater, which can produce enzymes that degrade wheat pentosan and improve the efficiency of wastewater utilization. Second, microbial fermentation produces a complex enzyme system during the biological modification process, which is more efficient than pure enzymatic modification.

In this study, wheat pentosan-degrading bacteria were selected from wheat starch wastewater and used to control the relative molecular weights of pentosans. Water-insoluble pentosans were converted into water-soluble pentosans, and improvements in the processability the pentosan chitosan film after modification were analyzed.

Results and Discussion

Screening of strains

A single colony for each strain was picked from a separation plate, transferred to a screening plate, and incubated at 37°C for 2 days. After the pentosan degraded, a transparent circle formed. The screening results are shown in Figure 1. Wheat pentosan was used as the only carbon source in the screening medium, which enabled screening for strains that use wheat pentosan.

Figure 1. Image of a strain obtained by screening

Oxford cup experiment

As shown in Figure 2A, “g” and “a” represent bacteria cultured on media containing different carbon sources that both produce enzymes capable of degrading wheat pentosan, indicating that the enzyme produced by the bacteria was not inducible. After fermentation, the supernatants of g and a, cultured with different carbon sources, also showed enzyme activity (Figure 2B). The results suggested that the related bacterial enzymes were produced in secreted form.

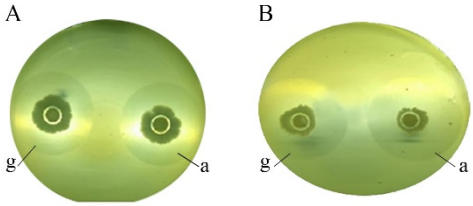

Figure 2. Strain and supernatant culture results. (A) Bacteria were cultured for 48 h. (B) Supernatants were cultured for 48 h. “g”: glucose was used as the sole carbon source in the medium; “a”: wheat pentose was used as the sole carbon source in the medium

Strain degrading pentosan activity

The bacterial strains, *yeast* cells, *B. subtilis* cells, and *B. licheniformis* cells were simultaneously inoculated into a screening plate. After 24 h of culture, only the α-strains showed transparent circles. After 48 h of culture, the phenomenon of transparent circles surrounding the α-strains became more obvious. As shown in Figure 3, wheat pentosan was barely degraded by the other strains. This finding showed that the obtained strain had high wheat pentosan degradation activity.

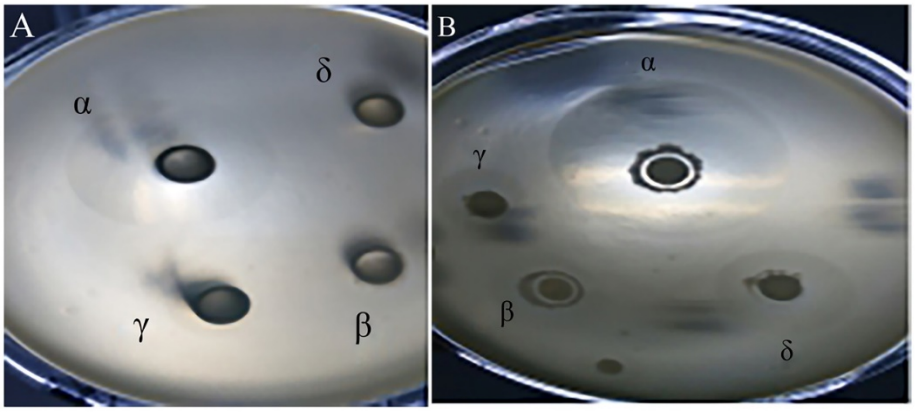

Figure 3. Results observed after culturing different strains. The bacteria shown in panels A and B were cultured for 24 and 48 h, respectively. (α) Screened strain (β) *B. subtilis* W800n, (γ) *B. licheniformis*, (δ) yeast

Strain identification

The strains were observed under a microscope with low- to high-magnification objectives. The results showed that this strain was gram-positive.

The bacterial 16S rDNA gene was sequenced, and the results showed that the 16S rDNA gene was 1452 base pairs long, consistent with the results of electrophoresis (Table 1).

BLAST analysis of the partial 16S rDNA gene was performed against sequences deposited in GenBank (Table 2). A multiple sequence alignment was performed based on the 16S rDNA BLAST results, using sequences with differing homology and originating from different bacteria. MEGA software (version 5.1) was used to construct a phylogenetic tree (Figure 2). The bacterium was named MXT-1.

Our results showed that strain MXT-1 shared a close relationship with *B. subtilis* strain 2C-62. The 16S rDNA gene was 99% homologous. The MXT-1 strain was subjected to comprehensive morphological and molecular biological analyses. Finally, the strain MXT-1 was classified as *B. subtilis*.

Table 1. Sequence of the 16S rDNA gene of the MXT-1 strain

1	GAATGGCGCG TGCCTATAAT GCAGTCGAGC GGACAGATGG GAAGCTCCGC TCCCTGATGT
61	TCGCGGCGGA CGGGTGTAGT AACACGTGGG TAACCTGCCT GTAAGACTGG GATAACTCCG
121	GGAAACCGGG GCTAATACCG GATGCTTGTT TGAACCGCAT GGTTCAAACA TAAAAGGTGG
181	CTTCGGCTAC CACTTACAGA TGGACCCGCG GCGCATTAGC TAGTTGGTGA GGTAACGGCT
241	CACCAAGGCG ACGATGCGTA GCCGACCTGA GAGGGTGATC GGCCACACTG GGACTGAGAC
301	ACGGCCCAGA CTCCTACGGG AGGCAGCAGT AGGGAATCTT CCGCAATGGA CGAAAGTCTG
361	ACGGAGCAAC GCCGCGTGAG TGATGAAGGT TTTCGGATCG TAAAGCTCTG TTGTTAGGGA
421	AGAACAAGTG CCGTTCAAAT AGGGCGGCAC CTTGACGGTA CCTAACCAGA AAGCCACGGC
481	TAACTACGTG CCAGCAGCCG CGGTAATACG TAGGTGGCAA GCGTTGTCCG GAATTATTGG
541	GCGTAAAGGG CTCGCAGGCG GTTTCTTAAG TCTGATGTGA AAGCCCCCGC TCAACCCGGG

```
601   GAGGGTCATT GGAAACTGGG GAACTTGAGT GCAGAAGAGG AGAGTGGAAT TCCACGTGTA
661   GCGGTGAAAT GCGTAGAGAT GTGGAGGAAC ACCAGTGGCG AAGGCGACTC TCTGGTCTGT
721   AACTGACGCT GAGGAGCGAA AGCGTGGGGA GCGAACAGGA TTAGATACCC TGGTAGTCCA
781   CGCCGTAAAC GATGAGTGCT AAGTGTTAGG GGGTTTCCGC CCCTTAGTGC TGCAGCTAAC
841   GCATTAAGCA CTCCGCCTGG GGAGTACGGT CGCAAGACTG AAACTCAAAG GAATTGACGG
901   GGGCCCGCAC AAGCGGTGGA GCATGTGGTT TAATTCGAAG CAACGCGAAG AACCTTACCA
961   GGTCTTGACA TCCTCTGACA ATCCTAGAGA TAGGACGTCC CCTTCGGGGG CAGAGTGACA
1021  GGTGGTGCAT GGTTGTCGTC AGCTCGTGTC GTGAGATGTT GGGTTAAGTC CCGCAACGAG
1081  CGCAACCCTT GATCTTAGTT GCCAGCATTC AGTTGGGCAC TCTAAGGTGA CTGCCGGTGA
1141  CAAACCGGAG GAAGGTGGGG ATGACGTCAA ATCATCATGC CCCTTATGAC CTGGGCTACA
1201  CACGTGCTAC AATGGGCAGA ACAAAGGGCA GCGAAACCGC GAGGTTAAGC CAATCCCACA
1261  AATCTGTTCT CAGTTCGGAT CGCAGTCTGC AACTCGACTG CGTGAAGCTG GAATCGCTAG
1321  TAATCGCGGA TCAGCATGCC GCGGTGAATA CGTTCCCGGG CCTTGTACAC ACCGCCCGTC
1381  ACACCACGAG AGTTTGTAAC ACCCGAAGTC GGTGAGGTAA CCTTTTTGGA GCCAGCCGCC
1441  GAAGTGACAG AG
```

139 **Table 2.** Homology analysis of 16S rDNA sequence of the MXT-1 strain

Accession number	Sequence description	Same-origin coverage (%)	Homology (%)
KR061403.1	*B. subtilis* strain 2C-62 16S ribosomal RNA gene, partial sequence	99	99
JN132107.1	*Bacillus* sp. Q2 16S ribosomal RNA gene, partial sequence	99	99
KP209408.1	*B. amyloliquefaciens* strain EB32 16S ribosomal RNA gene, partial sequence	99	99
CP009748.1	*B. subtilis* strain ATCC 13952, complete genome	99	99
KJ123715.1	*B. amyloliquefaciens* strain V3 16S ribosomal RNA gene, partial sequence	99	99
CP002634.1	*B. amyloliquefaciens* LL3, complete genome	99	99

CP002627.1	*B. amyloliquefaciens* TA208, complete genome	99	99
HQ153104.1	*B. subtilis* strain HFBL124 16S ribosomal RNA gene, partial sequence	99	99
AY881642.1	*B. subtilis* strain CICC10036 16S ribosomal RNA gene, partial sequence	99	99

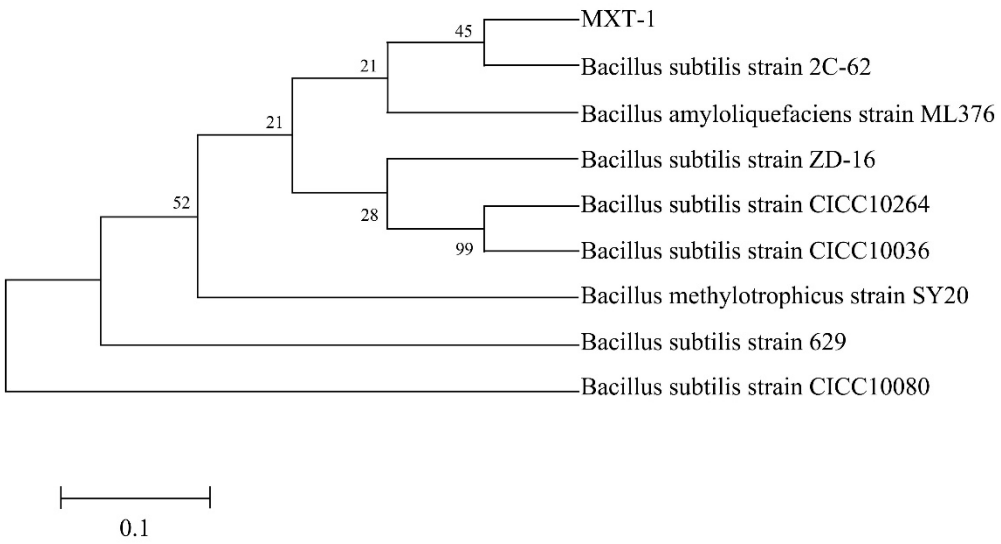

Figure 4. Phylogenetic map for the 16S rRNA gene of strain MXT-1

The MXT-1 strain selected in this study had high pentosan degradation activity, suggesting important roles in the degradation and efficient utilization of pentosan in nature.

Strain fermentation results

Figure 5 shows changes in total polysaccharides after 36 h of fermentation. The polysaccharide content also decreased. However, pentosan was slowly degraded by MXT-1 in the initial stage and accelerated in the intermediate stage.

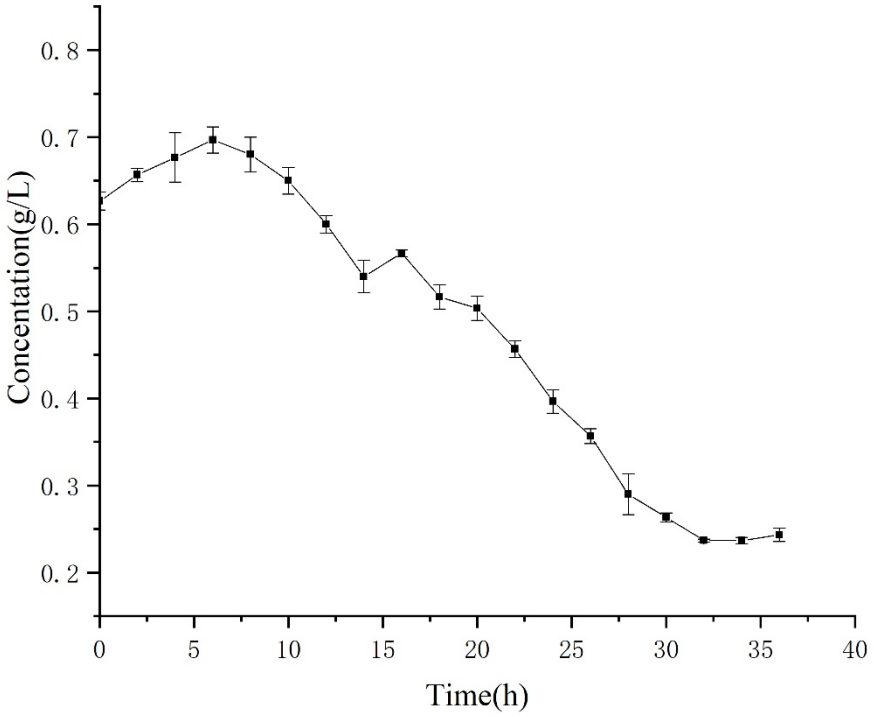

Figure 5. Wheat pentosan concentrations during fermentation

Table 3 shows the molecular weight of wheat pentosan varied with the bacterial-fermentation time. The relative molecular weight gradually decreased from 1730 to 257 kDa as the fermentation time increased to 22 h. Figure 6 shows the purification process of pentosan at different fermentation times. Some of the enzymes produced by the wheat pentosan-degrading bacteria can be secreted extracellularly by the MXT-1 strain. The endo-reaction of β-1,4 glycosidic bonds in wheat pentosan can lead to decreased polymerization. Enzymes acting on the side chains of pentosans may be produced by MXT-1, thereby reducing its branching and increasing its water solubility [17]. Previous findings have shown that the enzymatic degradation of pentosan generally depends on the synergistic effects of arabinofuranosidase and endoxylanase [18]. Therefore, the direct use of MXT-1 to degrade pentosan reduces production costs to a certain extent.

Table 3. Relative molecular weights of wheat pentosan after increasing fermentation times

Fermentation time (h)	Relative molecular weight (kDa)
0	1730

12	646
14	360
16	344
18	298
20	270
22	257

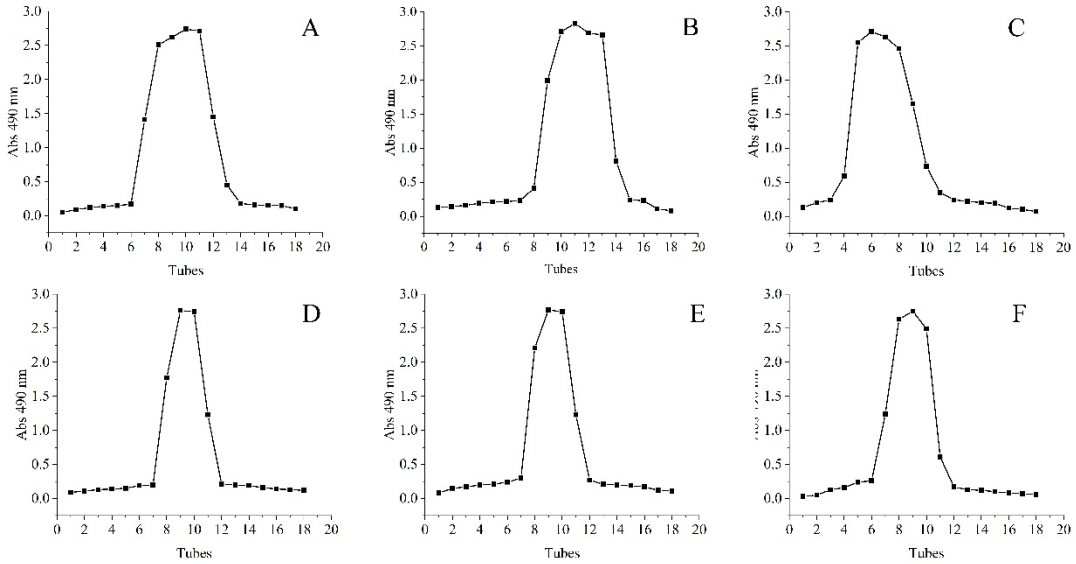

Figure 6. Purification curves for pentosan at different fermentation time. The graphs shown in panels A–F represent wheat pentosan recovered after fermentation for 12, 14, 16, 18, 20, or 22 h, respectively.

Characterization and performance of the composite film

Table 4 shows the WVP of the composite film materials before and after modification. The WVP was calculated according to Eq. (1). The WVP of the modified film material was significantly reduced. This finding may reflect better molecular compatibility between wheat pentosan and chitosan and stronger hydrogen bonding between the molecules. Part of the gap was filled with small pentosan molecules produced by degradation, and the membrane structure was denser. The chain arrangement of hydrogen bonds is enhanced by the flow of free low molecular-weight molecules between longer polymers [19]. In addition, a previous study showed that the free aldehyde group content in a pentosan solution increases after fermentation, making the film structure more compact [20]. The Maillard reaction between the amino groups of chitosan and the aldehyde groups of pentosan is strong, which reduces the amino group content [20].

Table 4. WVP parameters of the composite films

Project	Unmodified composite film	Modified composite film
WVP ($g \cdot mm \cdot [m^2 \cdot h \cdot kPa]^{-1}$)	0.2769	0.1286

Table 5 shows that the swelling ratio of the unfermented pentosan-chitosan composite film was 1.23, whereas that of the modified film was 1.45. Modification increased the number of hydrophilic groups. The lower molecular chains had more water-absorbing active sites than the higher chains. Our results are similar to those of previous studies [19, 21].

Table 5. The masses of the films before and after swelling

Project	Unmodified composite film	Modified composite film
Swelling capacity	1.23 ± 0.014	1.45 ± 0.017

Figure 7 shows the tensile properties of the composite film before modification (A) and after modification (B). Before modification, the tensile strength of the composite film was 18.69 MPa, with a maximum displacement of 1.69 mm. In contrast, the tensile strength of the modified composite film is lower than the former, which is reduced by 95%, but the tensile displacement increased. Thus, the film flexibility may have increased owing to the increased number of short-chain wheat pentosan molecules. Low-molecular-weight molecules enhance the mobility of pentosan and chitosan molecules. Previous investigators have drawn similar conclusions [19, 22]. Increased flexibility is beneficial for food packaging films.

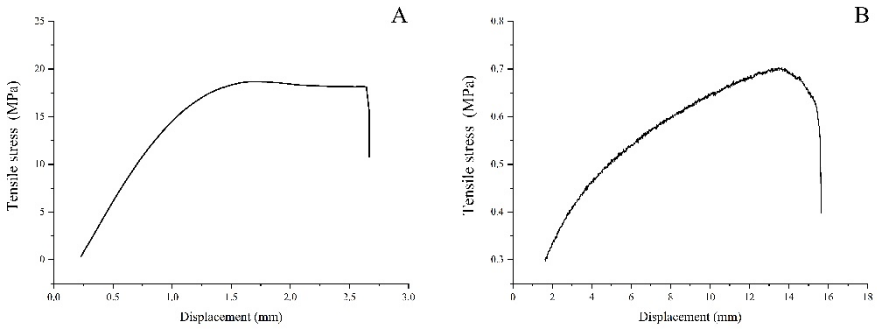

Figure 7. Tensile stress-displacement curves of the pentosan chitosan composite films. (A) Nonmodified pentosan chitosan composite films. (B) Pentosan chitosan composite films

Figure 8 shows FT-IR spectroscopy data indicating that wheat pentosan and chitosan molecules interacted before and after modification. Figure 8A shows an

absorption peak for the unmodified composite film at 2990 cm^{-1}, which was attributed to C–H stretching vibrations, and an absorption peak at 3456 cm^{-1}, which was attributed to O–H stretching vibrations. Figure 8B displays absorption peaks of the modified composite film at 2930 cm^{-1} (attributed to C–H stretching vibrations) and 3429 cm^{-1} (attributed to O–H stretching vibrations). After the modification, the hydroxyl-stretching vibration peak wave number of the membrane material decreased, and the peak shape widened. These results indicate that the modified pentosan/chitosan membrane material had stronger intermolecular hydrogen bonds and improved compatibility with polysaccharide molecules [21].

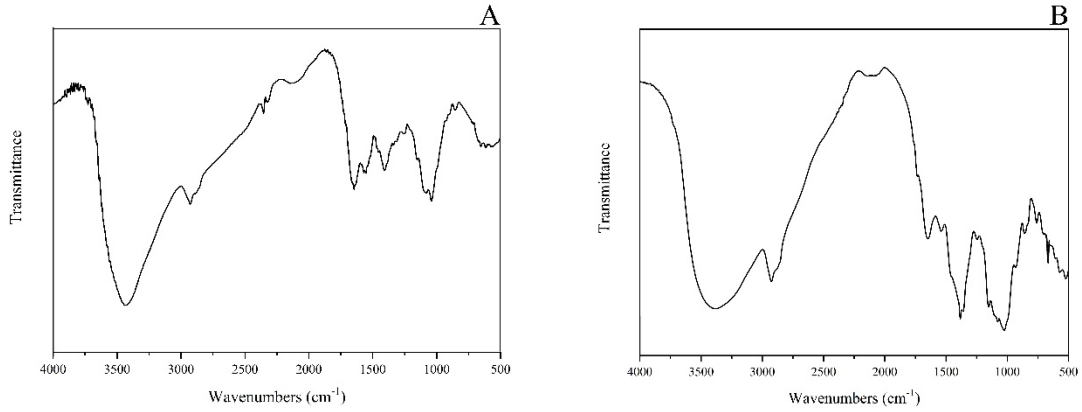

Figure 8. The FT-IR spectra of composite films. (A) Nonmodified pentosan chitosan composite films. (B) Modified pentosan chitosan composite films

The pentosan-modified chitosan surface morphology and cross-section of the composite film were determined by SEM, before and after modification. Figure 9A shows that the surface of the unmodified pentosan/chitosan composite film was smooth, and crystalline particles could only be observed at a magnification of 2000×. The surface of the film was flat, with no obvious wrinkles or bubbles. The surface of the modified composite film was rougher, which may reflect embrittlement during the liquid nitrogen treatment (Figure 9B). Figure 9C shows that the cross-sectional thickness of the unmodified composite film was uniform, but the texture was rough. Compared with Figure 9C, the results in Figure 9D illustrated that the cross-section thickness of the composite film after modification was uniform, the structure was more compact, and no obvious phase separation occurred. Similar SEM results were previously obtained for chitosan films containing cellulose and other polysaccharide composite films [21,23], which further confirmed that the modification increased the compatibility between the pentosan and chitosan molecules.

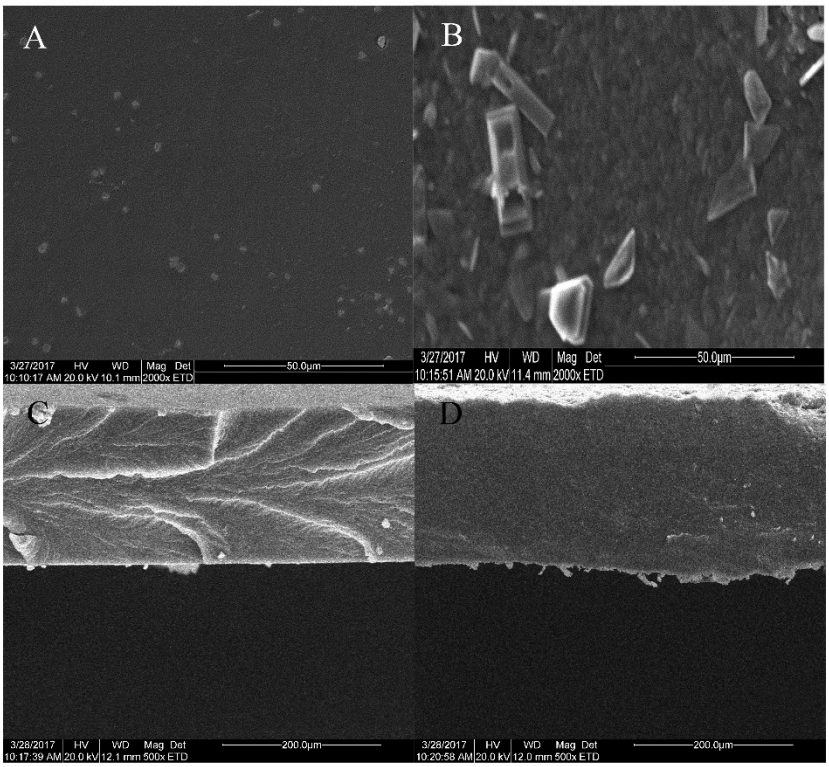

Figure 9. SEM micrographs of the surface and cross-section of pentosan chitosan films, before and after modification. (A, B) SEM surface images of pentosan chitosan composite films before and after modification. (C, D) SEM cross-sectional images of pentosan chitosan composite films, before and after modification

XRD is a method for analyzing the spatial structures of internal atoms. When the components of a polymer system are compatible, their interactions are strong, which changes their diffraction results. The diffraction curves of the two composite films in Figure 10A and 10B revealed diffraction peaks at 10–20°, although they were not particularly obvious. Figure 10A shows the diffraction pattern of the composite film before modification. The 2θ diffraction peaks appeared at 15.19° and 17.88°, and the characteristic diffraction peaks of chitosan appeared at approximately 10° and 20°. Figure 10B shows the diffraction pattern of the modified composite film. The 2θ diffraction peaks were observed at 15.74° and 21.09°. The diffraction peak of chitosan shifts to the higher 2θ direction. Chitosan has a semicrystalline structure [17]. After modification, the compatibility of pentosan and chitosan changed, which interfered with the crystallization. Similar results were reported previously [21].

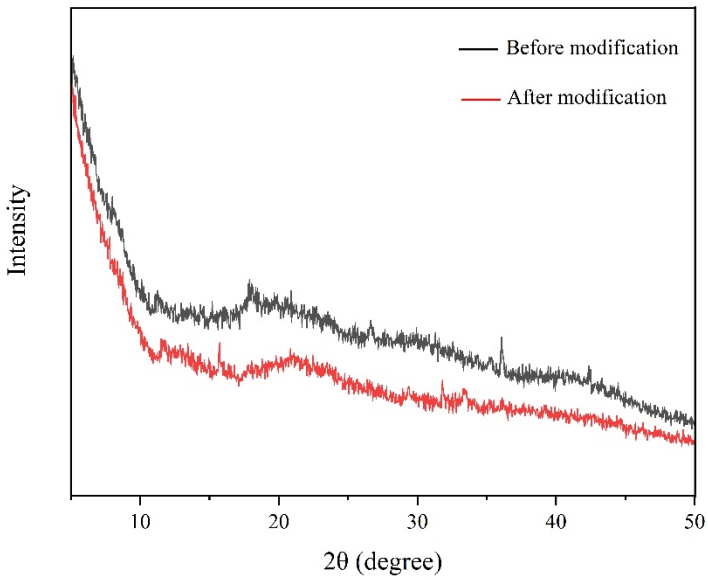

Figure 10. XRD spectra of composite films before and after modification. (A) Unmodified pentosan chitosan composite film. (B) Modified pentosan chitosan composite film

Conclusions

The physical properties of polysaccharide films can be improved by using strain MXT-1 to ferment and modify wheat pentosan. The enzyme system acting on the side chain of pentosan may be produced by MXT-1. The solubility of pentosan increased after biological modification, the compatibility between pentosan and chitosan molecules was improved, and hydrogen bonding was strengthened. The pores between the molecules were filled with small molecules produced by pentosan degradation, which improved the barrier properties of the film. The flexibility of the wheat pentosan composite film were improved, and the water vapor transmission rate was reduced. Furthermore, with a decrease in the molecular weight of pentosan, the tensile strength of the film decreased to a certain extent. Considering the health benefits of pentosans, the composite film is expected to become a good, edible food-preservation film. In the future, in order to develop a new type of smart food cling film with degradability, antibacterial properties, and green environmental protection, we will explore the effect of changing the concentration of pentosan and chitosan solution, the mixing ratio of pentosan and chitosan, and the molecular weight and structure of modified pentosan on the physical properties and antibacterial properties of the film.

Methods

Materials

Wheat B starch-wastewater samples were provided by Shandong Qufeng Food Tech

Co., Ltd. (Weifang, China). The composition analysis is presented in Table 6. Water-insoluble pentosans were extracted from wheat B starch wastewater according to Tao's method [24] and were found to have a relative molecular weight of 1730 kDa. 16S RNA primer synthesis and DNA sequencing were performed by Sangon Biotech Co., Ltd. (Shanghai, China). The DN11-Bacterial Genomic DNA Rapid Extraction Kit, PL03-High Purity Plasmid Small Amount Rapid Extraction Kit, DNA polymerase, DNA ligase, and *Escherichia coli* DH5α cells were purchased from Aidlab Biotechnologies Co., Ltd. (Beijing, China). The reagents used in this study were chemically pure. The name and composition of the culture medium involved in the experiment are shown in Table 7. All the medium ingredients were aseptically prepared.

Table 6. Wastewater composition analysis

Parameter	Result
Viscosity (mpa·s)	36
Solid content (%)	7.0
Glucose (%)	0.01
Protein (%)	0.43
Ash (%)	6.52

Table 7. The name and element of the culture medium

Name	Element ($g \cdot L^{-1}$)
Separation medium	Peeled potatoes 200, Glucose 20, KH_2PO_3, $MgSO_4$ 1.5, Agar 15, pH 6.0
Screening medium	KH_2PO_4 2, NH_4NO_3 2, $MgSO_4 \cdot 7H_2O$ 0.2, Yeast extract 5, Wheat pentosan 20, Agar 20, pH 6.0
Fermentation medium	Wheat pentosan 20, Yeast extract 5, KH_2PO_4 2, NH_4NO_2 2, $MgSO_4 \cdot 7H_2O$ 0.2, pH 6.0
LB medium	Yeast Dip Powder 5, Peptone 10, NaCl 10, pH 6.0
Medium with glucose as the sole carbon source	Glucose 20, KH_2PO_4 2, NH_4NO_3 2, $MgSO_4 \cdot 7H_2O$ 0.2, pH 6.0
Medium with wheat pentosan as the sole	Wheat pentosan 20, KH_2PO_4 2, NH_4NO_3 2, $MgSO_4 \cdot 7H_2O$ 0.2, pH 6.0

carbon source

Separation and screening of strains

One milliliter of sample solution was absorbed from the collected wheat B starch-production wastewater sample solution and diluted 10^{-3}-, 10^{-5}-, or 10^{-7}-fold [25]. An appropriate amount of each dilution was inoculated in separation medium and then incubated at 37°C for 2 days. The single colony on the separation plate was streaked across solid medium cultivated as described above, and the transparent circle was observed.

Oxford cup experiment

We verified the inducibility of wheat pentosan-degrading enzymes produced by the target strain. As shown in Table 7, glucose (g) and pentosan (a) were used as the sole carbon sources for the two media, respectively [26]. In a sterile environment, the selected strains were respectively inoculated into two media and cultured for an appropriate time. After the fermentation, the bacterial cells were washed several times with sterile water and made into a suspension. 200 μL of each prepared suspension was transferred into separate Oxford cuvettes and incubated at 28°C for 2 days. For the target strain, we observed whether a transparent circle was produced on the medium with non-pentosan as the carbon source to determine whether the pentosan-degrading enzyme produced by the bacteria was inducible. Additionally, we observed whether there was a transparent circle in the fermentation supernatant of the strain to verify whether the pentosan-degrading enzyme was secreted [27].

Degradation activity experiment of wheat pentosan by target strain

The activity of this strain was compared with that of other wheat pentosan-degrading strains. The bacterial strain, *β-B. subtilis* W800n, *γ-licheniformis*, *δ-yeasts* were cultured in LB medium. After 20 h, 200 μL of the same volume of the four cultured bacterial liquids was inoculated into four Oxford cuvettes on the same solid screening plate and incubated at 28°C for 2 days [27]. The results of culture were observed and compared.

Strain attributes and molecular biology identification

The morphology of the strain was observed, and the basic properties of the strain were verified by Gram staining [28]. Genomic DNA was extracted from the strain, and the target gene sequence was amplified. The genus of the strain was determined by performing Basic Local Alignment Search Tool (BLAST) analysis against sequences deposited in GenBank [29].

Wheat pentosan fermentation and molecular weight analysis

Drawing the growth curve of the strain

The strains were inoculated into the fermentation medium, the composition of the

medium is shown in Table 2. Samples were taken every 2 h, and the optical density at 600 nm (OD_{600}) was measured [30]. Three parallel experiments were performed, and the growth curves of the strains were drawn using Origin 8 based on the experimental results.

Determination of the wheat pentosan content during fermentation

The phenol-sulfuric acid method was used to monitor changes in the wheat pentosan content during fermentation [31]. Wheat pentosan exists in water-soluble and non-water-soluble forms. To increase the degradation effect of wheat pentosan, we first cultured the strain in LB medium containing 0.1% glucose until the OD_{600} exceeded 8.0, after which the cells were precipitated, washed, and cultured further on a shaker for 36 h. The pentosan-degradation process was monitored, and the fermentation broth was collected every 2 h. The pentosan content generated during fermentation was analyzed according to the phenol-sulfuric acid method.

Molecular weight analysis of wheat pentosan after fermentation

The molecular weight of the wheat pentosan was analyzed after fermentation. DEAE-cellulose 52 was used to purify and analyze the fermented wheat pentosan [32]. Sepharose-CL 6B chromatography was used to analyze the relative molecular-weight distribution. The phenol-sulfuric acid method was used to determine the polysaccharide contents in real time [33]. Dextrans with different relative molecular weights were collected, and standard curves were constructed [33]. A Sepharose-CL 6B column was used to analyze the relative molecular weights of the wheat pentosan species after fermentation.

Preparation of pentosan-chitosan composite films

Wheat pentosan and chitosan were used to prepare composite films. Wheat pentosan was suspended in water and stirred to obtain a wheat pentosan solution. Chitosan was added to a 1% acetic acid solution to prepare a 1.5% chitosan solution. Both solutions were mixed to obtain a mixed film solution [34]. The resulting solution was heated to 60–65°C, 1% glycerin was added as a plasticizer, and mixing was performed using magnetic stirring for 4 h. The film liquid was degassed by sonication for 10 min, cast onto a glass plate, and naturally dried at 23°C and 50% relative humidity (RH). The films were removed from the board for use.

A modified pentosan film solution was obtained after strain fermentation and used to prepare films by mixing biologically modified wheat pentosan with chitosan. The chitosan film solution was prepared according to the method described above. The performance of the two pentosan chitosan composite films before and after modification were analyzed [35].

Measuring the performance of the composite film

The water-vapor permeability (WVP) of each sample was measured according to

American Society for Testing and Materials standard 2005 [36]. Each film was sealed with an aluminum cup containing 43 g dry $CaCl_2$, and the cup was placed in an environment with 100% RH. A 6-mm air gap was present between the desiccant and the underside of the film. An aluminum cup was placed in a drying box with a fan. The fan circulated the air above the sample at rotated at a speed of 0.15 $m \cdot s^{-1}$. A saturated $Mg(NO_3)_2$ solution was used to maintain the temperature at 22°C while maintaining the RH at 100%. The cup was weighed several times over a period of 4 days, and the WVP was calculated using Eq. (1).

$$WVP = \frac{(m_2 - m_1) \times L}{A \times t \times \Delta P} \quad (1)$$

where WVP is the water-vapor permeability; m_1 and m_2 are the masses of the film, vapor-permeable cup, and $CaCl_2$ before and after water absorption, respectively; L is the thickness of the film; A is the effective measurement area; T is the measurement interval; and ΔP is the vapor-pressure difference on both sides of the film.

The water solubility of the films was tested as follows. Each dried film was cut into a size of 3 × 3 cm^2. An analytical balance was used to weigh the mass of each film three times in parallel, and the average value was recorded as m_1. The composite film was immersed in 50 mL distilled water for 24 h at 25°C until swelling equilibrium was reached. Filter paper was used to absorb water from the surface of the film material [37]. The mass was weighed three times, the average value of the swollen mass was recorded as m_2, and the water solubility was calculated according to Eq. (2) [38].

$$\text{Water solubility} = \frac{m_2 - m_1}{m_1} \quad (2)$$

where m_1 and m_2 are the masses of the film before and after swelling, respectively.

To determine the tensile strength of the films, the films were cut into strips with a width of 5 mm and length of 100 mm. Each strip of film was cut into three pieces for tensile testing. A universal testing machine (Instron 5943, Instron) was used to measure the mechanical properties at 23°C and 50% RH. The initial distance between the clamps was 50 mm, and a 0.3 N load cell was used for testing at 5 $mm \cdot min^{-1}$. The tensile strength and tensile displacement of the three test pieces were measured, and the average of the parallel test results was calculated [39].

Characterization of the pentosan-chitosan composite film

Fourier-transformed infrared (FT-IR) spectroscopy

FT-IR spectroscopy is a technique that detects chemical bonds in molecules by generating infrared absorption spectra of solids, liquids, or gases. An infrared spectrometer (IR Prestige-21, Shimadzu) was used to analyze the infrared spectra of the composite films before and after modification [40].

Film microstructure examination by scanning electron microscopy (SEM)

A Quanta 200 SEM instrument (Field Electron and Ion Company) was used to observe the microstructure of the surface and section of the wheat pentosan-chitosan composite

films, before and after biological modification [36].

Determination of the degree of crystallinity by X-ray diffraction

A D8-ADVANCE XRD instrument (AXS) used to determine the crystallinity of the wheat pentosan films, before and after biological modification [40].

Availability of data and materials

The datasets used and/or analysed during the current study are available from the corresponding author on reasonable request.

Competing interests

The authors declare that there are no competing interests.

Authors' contributions

Fei Zhao, Xiaofeng Wei, Xiangling Tao, and Piwu Li participated in the design of the study; Xiangling Tao carried out the major experiments; Fei Zhao drafted the manuscript; Feng Ding revised and improved important knowledge content; Feng Ding and Piwu Li reviewed and approved the final manuscript to be published.

Acknowledgments

We gratefully acknowledge the staff of the Qilu University of Technology (Shandong Academy of Sciences) for support and comments during the preparation of this manuscript. This work was supported by the Foundation of Qilu University of Technology of Cultivating Subject for Biology and Biochemistry [grant number 202001]. We would like to thank Editage (www.editage.cn) for English language editing.

References

[1] Siracusa V: Microbial Degradation of Synthetic Biopolymers Waste. Polymers (Basel) 2019, 11:1066.

[2] Costa MJ, Cerqueira MA, Ruiz HA, Fougnies C, Richel A, Vicente AA, Teixeira JA, Aguedo M: Use of wheat bran arabinoxylans in chitosan-based films: Effect on physicochemical properties. Industrial Crops and Products 2015, 66:305-311.

[3] Ying R, Li T, Wu C, Huang M: Preparation and characterisation of arabinoxylan and (1,3) (1,4)-β-glucan alternating multilayer edible films simulated those of wheat grain aleurone cell wall. International Journal of Food Science & Technology 2020, 56(7):3188-3196.

[4] Marcotuli I, Colasuonno P, Hsieh YSY, Fincher GB, Gadaleta A: Non-Starch Polysaccharides in Durum Wheat: A Review. Int J Mol Sci 2020, 21:2933.

[5] Zhang C, Ren H, Zhong C: Economical production of vitamin K2 using wheat starch wastewater. Journal of Cleaner Production 2020, 270:122486.

[6] Chen B, Li K, Liao L, Wang R, Li P: Ammonium Gluconate Production from

Potato Starch Wastewater Using a Multi-Enzyme Process. American Journal of Potato Research 2019, 96(5):447-456.

[7] Alvarez P, Alvarado C, Puerto M, Schlumberger A, Jimenez L, De la Fuente M: Improvement of leukocyte functions in prematurely aging mice after five weeks of diet supplementation with polyphenol-rich cereals. Nutrition 2006, 22(9):913-921.

[8] Li W, Hu H, Wang Q, Brennan CS: Molecular Features of Wheat Endosperm Arabinoxylan Inclusion in Functional Bread. Foods 2013, 2(2):225-237.

[9] Mendis M, Simsek S: Arabinoxylans and human health. Food Hydrocolloids 2014, 42:239-243.

[10] Mansberger A, D'Amico S, Novalin S, Schmidt J, Tömösközi S, Berghofer E, Schoenlechner R: Pentosan extraction from rye bran on pilot scale for application in gluten-free products. Food Hydrocolloids 2014, 35:606-612.

[11] Saxena A, Elder TJ, Kenvin J, Ragauskas AJ: High Oxygen Nanocomposite Barrier Films Based on Xylan and Nanocrystalline Cellulose. Nano-Micro Letters 2010, 2(4):235-241..

[12] Gröndahl M, Eriksson L, Gatenholm PJB: Material properties of plasticized hardwood xylans for potential application as oxygen barrier films. Gatenholm 2004, 5(4):1528-1535.

[13] Egues I, Stepan AM, Eceiza A, Toriz G, Gatenholm P, Labidi J: Corncob arabinoxylan for new materials. Carbohydrate Polymers 2014, 102:12-20.

[14] Peng P, Zhai MZ, She D, Gao YF: Synthesis and characterization of carboxymethyl xylan-g-poly(propylene oxide) and its application in films. Carbohydrate Polymers 2015, 133:117-125.

[15] Mikkonen KS, Rita H, Helen H, Talja RA, Hyvonen L, Tenkanen M: Effect of polysaccharide structure on mechanical and thermal properties of galactomannan-based films. Biomacromolecules 2007, 8(10):3198-3205.

[16] Izydorczyk M, Biliaderis C, Bushuk WJJoCS: Oxidative gelation studies of water-soluble pentosans from wheat. Bushuk 1990, 11(2):153-169.

[17] Romero-Garcia S, Hernandez-Bustos C, Merino E, Gosset G, Martinez A: Homolactic fermentation from glucose and cellobiose using Bacillus subtilis. Microb Cell Fact 2009, 8:23.

[18] Goncalves TA, Damasio AR, Segato F, Alvarez TM, Bragatto J, Brenelli LB, Citadini AP, Murakami MT, Ruller R, Paes Leme AF et al: Functional characterization and synergic action of fungal xylanase and arabinofuranosidase for production of xylooligosaccharides. Bioresour Technol 2012, 119:293-299.

[19] Cheng LH, Abd Karim A, Seow CC: Effects of acid modification on physical properties of konjac glucomannan (KGM) films. Food Chemistry 2007, 103(3):994-1002.

[20] Umemura K, Kawai S: Preparation and characterization of Maillard reacted chitosan films with hemicellulose model compounds. Journal of Applied Polymer Science 2008, 108(4):2481-2487.

[21] Luo A, Hu B, Feng J, Lv J, Xie S: Preparation, and physicochemical and

biological evaluation of chitosan-Arthrospira platensis polysaccharide active films for food packaging. J Food Sci 2021, 86(3):987-995.

[22] Leceta I, Guerrero P, de la Caba K: Functional properties of chitosan-based films. Carbohydr Polym 2013, 93(1):339-346.

[23] Indriyati, Dara F, Primadona I, Srikandace Y, Karina M: Development of bacterial cellulose/chitosan films: structural, physicochemical and antimicrobial properties. Journal of Polymer Research 2021, 28:70.

[24] Tao X, Li P, Chen B, Response surface analysis for the optimization of the alkali extraction technology of water insoluble pentosan from the wheat gluten waste water. Food Science and Technology, 2017, 42:06.

[25] Liu S, Zhang Y, Zeng P, Wang H, Song Y, Li J: Isolation and Characterization of a Bacterial Strain Capable of Efficient Berberine Degradation. Int J Environ Res Public Health 2019, 16:646.

[26] Sachan P, Madan S, Hussain A: Isolation and screening of phenol-degrading bacteria from pulp and paper mill effluent. Applied Water Science 2019, 9:100.

[27] Swamy P: Laboratory manual on biotechnology: Rastogi Publications; 2008.

[28] Hiremath P, Bannigidad PJIJoBE, Technology: Automated Gram-staining characterisation of bacterial cells using colour and cell wall properties. Technology 2011, 7(3):257-265.

[29] Ye GB, Hong MH, Huang D, Yang XD: Identification and Primary Application of Two High-Yield Glucoamylase Moulds from Luzhou-Flavor Daqu. Advanced Materials Research 2013, 781-784:1825-1829.

[30] Panda I, Balabantaray S, Sahoo SK, Patra N: Mathematical model of growth and polyhydroxybutyrate production using microbial fermentation of Bacillus subtilis. Chemical Engineering Communications 2017, 205(2):249-256.

[31] Kim H, Hong HD, Shin KS: Structure elucidation of an immunostimulatory arabinoxylan-type polysaccharide prepared from young barley leaves (Hordeum vulgare L.). Carbohydr Polym 2017, 157:282-293.

[32] Prashanth MRS, Muralikrishna G: Arabinoxylan from finger millet (Eleusine coracana, v. Indaf 15) bran: Purification and characterization. Carbohydrate Polymers 2014, 99:800-807.

[33] Le Gall M, Eybye KL, Knudsen KEB: Molecular weight changes of arabinoxylans of wheat and rye incurred by the digestion processes in the upper gastrointestinal tract of pigs. Livestock Science 2010, 134(1-3):72-75.

[34] Souza MP, Vaz AFM, Silva HD, Cerqueira MA, Vicente AA, Carneiro-da-Cunha MG: Development and Characterization of an Active Chitosan-Based Film Containing Quercetin. Food and Bioprocess Technology 2015, 8(11):2183-2191.

[35] Xiang Z, Watson J, Tobimatsu Y, Runge T: Film-forming polymers from distillers' grains: structural and material properties. Industrial Crops and Products 2014, 59:282-289.

[36] Lin D, Kuang Y, Chen G, Kuang Q, Wang C, Zhu P, Peng C, Fang Z:

549 Enhancing moisture resistance of starch-coated paper by improving the film forming
550 capability of starch film. Industrial Crops and Products 2017, 100:12-18.
551 [37] Wang S, Ren J, Li W, Sun R, Liu S: Properties of polyvinyl alcohol/xylan
552 composite films with citric acid. Carbohydr Polym 2014, 103:94-99.
553 [38] Yoon S-D, Chough S-H, Park H-R: Preparation of resistant starch/poly(vinyl
554 alcohol) blend films with added plasticizer and crosslinking agents. Journal of
555 Applied Polymer Science 2007, 106(4):2485-2493.
556 [39] Alekhina M, Mikkonen KS, Alen R, Tenkanen M, Sixta H:
557 Carboxymethylation of alkali extracted xylan for preparation of bio-based packaging
558 films. Carbohydr Polym 2014, 100:89-96.
559 [40] Liu M, Zhou Y, Zhang Y, Yu C, Cao S: Preparation and structural analysis of
560 chitosan films with and without sorbitol. Food Hydrocolloids 2013, 33(2):186-191.
561
562